E2F1 promotes, JNK and DIAP1 inhibit, and chromosomal position has little effect on radiation-induced Loss of Heterozygosity in *Drosophila*

Jeremy Brown[1] and Tin Tin Su[2,3]

Department of Molecular, Cellular and Developmental Biology, 347 UCB,
University of Colorado, Boulder, CO 80309-0347

[1] University of Colorado, Anschutz Medical Campus, 13001 E. 17th Pl., Aurora, CO 80045

[2] University of Colorado Cancer Center, Anschutz Medical Campus, 13001 E. 17th Pl., Aurora, CO 80045

[3]Corresponding author: tin.su@colorado.edu

Short title: Radiation-induced genome instability

Keywords: *Drosophila*, radiation, loss of heterozygosity

Abstract

Loss of Heterozygosity (LOH) can occur when a heterozygous mutant cell loses the remaining wild type allele to become a homozygous mutant. LOH can have physiological consequences if, for example, the affected gene encodes a tumor suppressor. We used two fluorescent reporters to study mechanisms of LOH induction by X-rays, a type of ionizing radiation (IR), in *Drosophila* larval wing discs. IR is used to treat more than half of cancer patients, so understanding its effects is of biomedical relevance. Quantitative analysis of IR-induced LOH at seven different positions between the telomere and the centromere, the first such study that we know of, showed that while a homologous chromosome is required to produce LOH after irradiation, position along the chromosome makes little difference. This suggests that IR-induced LOH occurs via non-recombination-based mechanisms, unlike what was previously reported for spontaneously occurring LOH. Using a focused screen, we identified E2F1 as a key promotor of LOH and further testing suggests a mechanism involving its role in cell cycle regulation rather than apoptosis. We leveraged the loss of a transcriptional repressor through LOH to express transgenes specifically in cells that have already acquired LOH. This approach identified JNK signaling and apoptosis as key determinants of LOH maintenance. These studies reveal previously unknown mechanisms for generation and elimination of cells with chromosome aberrations after exposure to IR.

Summary

Loss of Heterozygosity (LOH) can lead to homozygous mutant cells, with potential physiological consequences if it affects tumor suppressor genes. Using fluorescent reporters of LOH in *Drosophila* wing discs, we found that X-ray-induced LOH requires a homologous chromosome but was unaffected by position along the chromosome. This suggests non-recombination mechanisms for X-ray-induced LOH, unlike spontaneous LOH. We found that E2F1 promotes LOH while JNK signaling and apoptosis eliminates cells with LOH, uncovering new insights into chromosomal aberrations post-exposure to radiation.

48 **Introduction**

49 Loss of Heterozygosity (LOH) occurs when a heterozygous cell loses an allele to become
50 homozygous. LOH can have physiological consequences if, for example, the lost allele encodes a
51 tumor suppressor. Possible mechanisms for LOH include mutations in the gene, aneuploidy of
52 whole or segments of chromosomes, and mitotic recombination between the locus and the
53 centromere (producing -/- and +/+ twin spots from a -/+ cell). We are using *Drosophila*
54 *melanogaster* as a model to study LOH that follows exposure to X-rays, a type of ionizing
55 radiation (IR). IR causes DNA strand breaks and its ability to induce apoptosis is the reason IR is
56 used to treat half of cancer patients. Understanding IR's effects on genome integrity is a crucial
57 step towards rendering radiation therapy safe.
58
59 Classical and recent studies of IR-induced LOH in *Drosophila* employed visible adult markers
60 such as *multiple wing hair* (*mwh*) and *forked (f)* that alter the number or morphology of actin-
61 based hairs on the cell surface (Baker *et al.* 1978). Starting with heterozygotes of recessive
62 alleles, induced homozygosity is detectable on a cell-by-cell basis. In these studies, exposure to
63 IR occurred in the larval stages while the resulting LOH was scored many days later in the adult.
64 To be able to monitor steps in between, we have been developing fluorescent LOH reporters
65 that can be used at all developmental stages.
66
67 In our published work (Brown *et al.* 2020), we used the QF/QS module wherein QF binds its
68 recognition sequence QUAS to promote transcription while QS represses QF (Riabinina *et al.*
69 2015). psc-QF drives the expression of QUAS-tdTomato (Tom) throughout the larval wing disc
70 (Fig 1A) unless repressed by ubiquitously-expressed QS^{9B} inserted at 100E1 on chromosome 3
71 (Fig 1F). Loss of QS^{9B} by LOH results in de-repression of QF and cell-autonomous Tom
72 expression (Fig 1C-C'). Our published study produced a surprising result; IR-induced *mwh* LOH
73 was lower by more than 10-fold compared to IR-induced QS^{9B} LOH detected under identical
74 experimental conditions in adult wings (Brown *et al.* 2020). Classical studies suggest that
75 segmental aneuploidy (loss of a chromosome segment) is the primary mechanism for IR-
76 induced LOH (Baker *et al.* 1978). If breakage and loss of the corresponding chromosome tip is
77 indeed the mechanism, *mwh* LOH would accompany the loss of more genes compared to QS^{9B}
78 LOH because *mwh* is further from the telomere than QS^{9B} (Fig 1F). Resulting *mwh* LOH cells may
79 be less fit than QS^{9B} LOH cells, explaining the difference in IR-induced LOH incidence we saw.
80 Alternatively, homozygous mutants for *mwh*, which encodes an actin-bundling protein, may be
81 less fit while the loss of QS, which has no known role in *Drosophila*, may be neutral and it is this
82 difference in gene function rather than the amount of chromosome lost that explains the
83 differences in IR-induced LOH incidence. To address these possibilities and to identify regulators
84 of IR-induced LOH, we studied the LOH incidence of six additional insertion loci (Fig 1F) and
85 performed a focused genetic screen.

86
87 **Results**
88 *IR-induced LOH shows sex-dependence but locus-independence*
89 We used 4000 Rads (R) of X-rays, a typical dose in *Drosophila* (for example, (BRODSKY *et al.* 2004;
90 WELLS AND JOHNSTON 2012)) because it kills more than half of the cells in wing discs, yet larvae
91 can still develop into viable adults. Thus, 4000R causes significant damage but is still compatible
92 with recovery and regeneration. To ask if the distance from the chromosome tip matters, we
93 studied QS^{5A} that is further from the telomere than QS^{9B} or *mwh* (Fig 1F). As for QS^{9B} (BROWN *et*
94 *al.* 2020), LOH for QS^{5A} is IR-dependent (Fig 2A-B). More important, QS^{9B} and QS^{5A} did not differ
95 significantly in IR-induced LOH clone number (Fig 2A) or clone area (Fig 2B). In feeding 3rd instar
96 larval stage, cells of the wing disc that will ultimately form the adult structures are in a single
97 layer columnar epithelium with uniform cell size. Therefore, clone area serves as a proxy for cell
98 number as in previous studies (BROWN *et al.* 2020). We normalize clone number and area to the
99 total disc area so that we can control for variations in disc size/total cell number. We conclude
100 that distance from the chromosome tip did not affect IR-induced LOH incidence.
101
102 The conclusion above is further supported by the study of GAL80 insertions at 5 loci along the X
103 chromosome that was used before to detect spontaneous (without IR) LOH (Fig 1B,D,F) (SIUDEJA
104 *et al.* 2015). For four of the five GAL80 insertions, wing discs from un-irradiated larvae show
105 very few cells with GFP signal that is as bright as what is seen after IR (Fig 2C-D, Supplemental
106 Fig 1). Occasional cells with faint GFP (arrow in Supplemental Fig 1A-A'') are consistent with a
107 recent report of spontaneous GAL80 'loss' in larval brains through poorly understood
108 mechanisms (GOUPIL *et al.* 2022). Importantly, we noticed in early experiments with GAL80 that
109 approximately half of the irradiated discs lacked GFP expressing clones. This is different from
110 what we saw with QS; for example, 32 of 38 QS^{9B} discs had Tom+ cells in Fig 2A '9B+IR' dataset.
111 QS insertions are on autosomes while GAL80 insertions are on the X chromosome. This led us to
112 hypothesize a sex-dependence in GAL80 LOH, like what was reported for spontaneous LOH of
113 X-linked loci (SIUDEJA *et al.* 2015). Analysis of wing discs from males and female larvae (see
114 Methods) show that IR-induced increases in GFP+ cells were confined almost exclusively to
115 females (Fig 2E-F).
116
117 The exception is the 12C insertion, which shows the greatest incidence of GFP+ cells without IR
118 via unknown mechanisms, and a further increase after IR (Fig 2G-H). Even in this case, IR
119 induced increase was significant only in the females (Fig 2I-L, quantified in G-H). Thus, IR-
120 induced GAL80 LOH shows sex-dependence for all five insertions, similar to the case for
121 spontaneous LOH (SIUDEJA *et al.* 2015). To our surprise, however, IR-induced LOH did not
122 decrease with proximity to the centromere. This is unlike spontaneous LOH (SIUDEJA *et al.* 2015);
123 $GAL80^{5B}$ showed spontaneous LOH in 75% of adult *Drosophila* intestines while the

124 corresponding number for GAL80^{19E} was 40%. In contrast, IR-induced LOH incidence was nearly
125 identical for GAL80^{5B} and GAL80^{19E} (Fig 2E-F, p=0.193 for clone number and 0.861 for clone
126 area). We conclude that IR-induced LOH shows sex-dependence (like spontaneous LOH) but
127 chromosomal position independence (unlike spontaneous LOH). Possible explanations are in
128 the Discussion.
129
130 *A focused screen identified E2F1 as a regulator of LOH*
131 Results so far address cis-acting determinants, namely, chromosome position of the LOH loci
132 and the presence of a homologous X chromosome. To identify trans-acting regulators, we
133 performed a focused screen through known regulators of DNA damage and stress responses,
134 cell growth, cell survival and cell competition (Supplemental Table 1), using published
135 constructs that have been shown to produce a phenotype, when possible. We used QS in this
136 screen so that we can use the GAL4/UAS system in parallel to knock down/overexpress genes.
137 We used QS^{9B} because it shows more robust IR-induced LOH incidence than QS^{5A}.
138
139 Transgenes were expressed in the posterior (P) half of wing discs using the protocol in Fig 1E. As
140 stated above, we saw no Tom clones without IR; therefore, only +IR data are shown (Fig 3 and
141 Supplemental Fig 2). Three controls were used: the TRiP III line that was the recipient of many
142 RNAi constructs and RNAi for the w gene (both as controls for RNAi) and w^{1118} (control for
143 overexpression or OE). After normalizing to compartment area to control for differences in
144 compartment size, IR-induced LOH clone number or area are not significantly different between
145 A and P compartments in all three controls (Fig 3A-B and Supplemental Fig 2). Most genes
146 tested did not affect IR-induced LOH including those with known roles in cell competition such
147 as duox and Xrp1 (Supplemental Fig 2). This group is of interest because a prior publication
148 suggested that cells with segmental aneuploidy, a possible mechanism for LOH generation, may
149 be eliminated by cell competition (McNamee and Brodsky 2009). We interpret negative results
150 with caution, however, because our protocol for conditional and transient expression (Fig 1E)
151 may not deplete gene function sufficiently even if the same construct produced a phenotype
152 under different expression conditions before.
153
154 The screen found mild effects with RNAi against Chk2 or Myc and with overexpression of
155 oncogenic Ras^{V12} (Fig 3A-B). Specifically, Chk2 RNAi increased LOH clone number while Myc
156 RNAi and Ras^{V12} decreased LOH clone number. The effect sizes, however, were small (1.5 to 2-
157 fold) and clone area was not significantly affected, suggesting compensating changes in the size
158 of individual clones. In addition, expression of Ras^{V12} in the P compartment produced epithelial
159 folds in both compartments in irradiated discs (Fig 3D-D'), making the quantification of clone
160 area challenging. Because of this and small effect sizes, we have not followed up on Chk2, Myc
161 and Ras.

162
163 In contrast, RNAi against E2F1 profoundly affected both LOH clone number and clone area with
164 a reduction of the former by 6-fold and the latter by more than 10-fold (Fig 3C, quantified in A-
165 B). *Drosophila* E2F1, like its mammalian homologs, promotes cell proliferation by promoting
166 G1/S transition via activation of cyclin E expression and G2/M transition via activation of
167 $Cdc25^{String}$ (REIS AND EDGAR 2004). E2F1 also promotes IR-induced apoptosis in the wing discs
168 when p53 has been depleted; that is, its role in apoptosis is negligible in a wild type background
169 (WICHMANN *et al.* 2006). Therefore, we addressed the more likely possibility that the
170 requirement for E2F1 in LOH clone formation/maintenance is through its role in the cell cycle.
171 To this end, we expressed Cdk inhibitors Dap and Rux to inhibit G1/S and G2/M transitions,
172 respectively, using the same temperature shift protocol as in Fig 1E. Both Dap and Rux
173 phenocopied E2F1 RNAi (Fig 3A-B), supporting the idea that the role of E2F1 is to promote the
174 proliferation of cells with LOH.
175
176 We normalize LOH clone number and area to the compartment area. If E2F1 depletion or
177 Dap/Rux overexpression in the P compartment affected all cells within this compartment
178 equally regardless of their LOH status, we should see little change in <u>normalized</u> LOH clone
179 number or area. Yet, we see multiple-fold reductions by both measures. We infer that
180 manipulations of cell cycle regulators have a more severe effect on cells with LOH than on cells
181 in the rest of the P compartment. Greater sensitivity of LOH cells to cell cycle inhibition is a new
182 finding.
183
184 The manipulations thus far alter gene expression in the whole compartment and identified
185 differential effects on LOH versus non-LOH cells. To address cell-autonomous needs in LOH cells
186 more directly, we took advantage of QS loss and consequent QF de-repression to express
187 QUAS-transgenes and assayed their effect. This protocol has the added advantage of identifying
188 needs AFTER the clones have formed and have initiated QF-mediated gene expression. As
189 proof-of-concept, we used a published QUAS-rpr transgene (PEREZ-GARIJO *et al.* 2013) to express
190 this pro-apoptotic gene specifically in LOH clones, with the expectation that such clones will be
191 lost to cell death. The results show the system works as expected; QUAS-rpr reduced both clone
192 number and clone area to near completion (Fig 4A-B, quantified in E-F).
193
194 Using QUAS-transgenes, we tested the role of JNK and apoptotic signaling in maintaining cells
195 with LOH. We first assessed transgene functionality by ubiquitous expression with psc-QF
196 (without QS) and assaying for expected phenotypes. For rpr, dominant negative bsk (JNK) and
197 puc (phosphatase and JNK inhibitor), we found lines that produced significant lethality
198 (Supplemental Table 2). For *Drosophila* Inhibitor of Apoptosis Protein 1 (DIAP1), even the
199 strongest effect on lethality was modest, so we assayed for inhibition of apoptosis instead. Of

200 three lines tested, 12M reduced IR-induced cleaved Dcp1 signal to near completion (Fig 4H),
201 14F showed a modest effect (Fig 4I), and 3M showed variable effect from disc to disc.
202 Therefore, QUAS-DIAP1 12M line was used in subsequent experiments. The results show that
203 cell-autonomous inhibition of JNK or apoptosis in cells with LOH led to a significant increase in
204 both Tom clone number and area. We conclude that in cells that survived LOH long enough to
205 activate QUAS-transgenes, stress signaling continues to operate to eliminate them.
206
207 **Discussion**
208 We report here studies on the role of chromosomal position and trans-acting regulators on IR-
209 induced LOH in *Drosophila* larval wing discs. We found that position along the chromosome
210 makes little difference while the presence of a homologous chromosome is required. We
211 identified E2F1 as a positive regulator of LOH clone incidence and propose that cells with LOH
212 are more sensitive to inhibition of cell proliferation than their neighbors. And we identified JNK
213 signaling and apoptosis as cell-autonomous mechanisms that eliminate cells that survived LOH
214 induction. This contrasts with the previous finding that JNK plays only a backup role in reducing
215 IR-induced *Minute* (M/+) bristles, a role that becomes apparent only in p53 mutant background
216 (McNamee and Brodsky 2009).
217
218 Spontaneous LOH in the adult *Drosophila* intestine is attributed to mitotic recombination,
219 based on several lines of evidence. First, sex-dependence is interpreted as arising from
220 recombination-based mechanisms that require the presence of a homologous chromosome
221 such as crossing over, gene conversion or break-Induced replication (Siudeja *et al.* 2015).
222 Second, adult guts with spontaneous GAL80^{5B} LOH was about twice as frequent as those with
223 spontaneous GAL80^{19E} LOH. An increase in LOH with distance from the centromere is predicted
224 for recombination-based mechanisms because a distal locus would experience more frequent
225 exchanges between homologous chromosomes. This study noted, however, that the frequency
226 of spontaneous LOH at 19E was higher than predicted from meiotic maps and higher than
227 observed for a centromere-proximal locus on chromosome 3R, suggesting additional factors at
228 play. Third, whole genome sequencing confirmed that spontaneous LOH of chromosome 2 loci
229 in the adult intestine occur through mitotic recombination (Zouabi *et al.* 2022).
230
231 Our finding that IR-induced LOH clone number and area were nearly identical for GAL80^{5B} and
232 GAL80^{19E} cannot be explained by recombination-based mechanisms. Classical studies by Baker
233 and others monitored several adult visible markers such as *yellow (y)* and *forked (f)* in
234 heterozygous adult females that were irradiated as larvae or pupae with 1000 R from a Co-60
235 source (Baker *et al.* 1978). In adult female abdomens monitored for *y* or *f*, both X-linked genes,
236 40% of LOH clones induced by IR (i.e., the difference between -/+IR samples) consisted of 40%
237 twin clones (likely products of mitotic recombination) while the remaining 60% were single

238 clones. Examination of single clones that arose spontaneously (without radiation) in the same
239 study found that 20% of cells in such clones showed *Minute* bristles, which result from
240 haploinsufficiency of loci encoding ribosomal proteins. The authors suggest that single LOH
241 clones arose by aneuploidy that turned wild type (+/+) cells into heterozygotes for ribosomal
242 protein genes (M/+). In another set of studies, McNamee and Brodsky used the *Minute* bristle
243 phenotype and assayed gain-of-heterozygosity, from +/+ to M/+, rather than loss-of-
244 heterozygosity, in bristles from adults that result from irradiated larvae (McNamee and Brodsky
245 2009). Recombination-based mechanisms induced by IR would not be detectable in this assay
246 as it would change +/+ to +/+. Regardless, taken together, these results suggest that both
247 aneuploidy and recombination-based mechanisms operate to produce IR-induced LOH in
248 tissues that produce the adult body wall. Our data suggest a greater contribution by non-
249 recombination-based mechanisms, namely aneuploidy.
250
251 Studies by Baker, Brodsky and colleagues did not distinguish among various types of
252 aneuploidies, which could include loss of whole or segments of chromosomes and terminal
253 deletions. Over-expression of telomere capping protein HipHop has been shown to increase the
254 survival of cells with terminal deletions that result from dividing experimentally induced
255 dicentric chromosomes (Kurzhals *et al.* 2017). Overexpression of HipHop, however, did not
256 increase the incidence of IR-induced LOH (Supplemental Fig 2), suggesting that terminal
257 deletions may not be the mechanism. The finding that distance from the telomere did not
258 affect the QS LOH incidence supports this idea. Instead, relevant types of aneuploidy may
259 include X-ray-induced segmental losses that are well-documented in numerous studies in
260 *Drosophila* and mammals (for example, (Pastink *et al.* 1987; Pastink *et al.* 1988; Eeken *et al.*
261 1994; Chick *et al.* 2005)). Such losses can explain our finding that LOH of X-linked loci requires a
262 homologous chromosome. We suggest that without part or whole of the X chromosome in XY
263 males, a cell may not survive to express GFP, reducing the level of LOH observed in males. In
264 other words, presence of one X chromosome allows cells to survive with partial or complete
265 loss of the other X chromosome.
266
267 **Materials and Methods**
268 *Drosophila stocks and methods*
269 *Drosophila* stocks used are in Supplemental Table 1 and include those with UAS-puc (Martin-
270 Blanco *et al.* 1998), UAS-Wg (Lawrence *et al.* 1996) and recombinant chromosome 3 encoding
271 tub-QS^{9B} and tub-GAL80^{ts} (Brown *et al.* 2020). QUAS lines are a gift from Ainhoa Pérez-Garijo
272 and Hermann Steller (Perez-Garijo *et al.* 2013). Virgin females and males were crossed and
273 cultured for three days on Nutri-Fly German Formula food (Genesee Scientific) at 25°C before
274 egg collections. Eggs were collected and larvae were raised on Nutri-Fly Bloomington Formula
275 food (Genesee Scientific) at 25°C unless otherwise noted. The cultures were monitored daily

276 for signs of crowding, typically seen as 'dimples' in the food surface, and were split as needed.
277 Larvae in food were placed in petri dishes and irradiated in a Faxitron Cabinet X-ray System
278 Model RX-650 (Lincolnshire, IL) at 115 kVp and 5.33 rad/sec. Larval sex was determined using
279 gonad size observed under a dissecting microscope; male gonads are large and free of the fat
280 body while female gonads are hard to find (KERKIS 1931).
281
282 *Tissue preparation and imaging*
283 Larval wing discs were dissected in PBS, fixed in 4% para-formaldehyde (PFA) in PBS for 30 min,
284 and washed three times with PBTx (0.1% Triton X-100). The discs were stained with 10 μg/ml
285 Hoechst33342 in PBTx for 5 min, washed 3 times, and mounted on glass slides in Fluoromount
286 G (SouthernBiotech). Wing discs were imaged on a Leica DMR compound microscope using a Q-
287 Imaging R6 CCD camera and Ocular or Micro-Manager software.
288
289 *Statistical Analysis*
290 For sample size justifications, we used a simplified resource equation from (CHARAN AND
291 KANTHARIA 2013); E = total number of animals − total number of groups, where E value of 10-20
292 is considered adequate. When we compare two groups (-IR and +IR, for example, where the
293 former is the control group and the latter is the treated group), n = 6 per group, or E = 11,
294 would be adequate. All samples subjected to statistical analysis meet or exceed this criterion.
295 To compute p-values, 2-tailed Student t-tests were used.
296
297 **Data and Reagent Statement**
298 Drosophila stocks are available upon request. The authors affirm that all data necessary for
299 confirming the conclusions of the article are present within the article, figures, and tables.
300
301 **Acknowledgments**
302 We thank the Perrimon, Bardin and Steller labs for fly stocks. Additional stocks from the
303 Bloomington *Drosophila* Stock Center (NIH P40OD018537) and Vienna *Drosophila* Resource
304 Center were used in this study.
305
306 **Funding**
307 This work was supported by the National Institutes of Health grant R35 GM130374 to TTS.
308

309 **Figure and Table Legends**

310

311 **Fig 1. Fluorescent reporters for loss-of-heterozygosity**

312 A. Loss of QS results in de-repression of psc-QF-driven Tom expression.

313 B. Loss of GAL80 results in de-repression of act-GAL4-driven GFP expression.

314 C-C'. An example of a wing disc with a Tom clone. This disc also expresses en-GAL4>GFP
315 that was used to express RNAi and transgenes in the posterior compartment of the disc. The
316 genotype was en-GAL4>UAS-GFP, psc-QF>Tom, QS^{5A}/+ from the cross of en-GAL4>UAS-GFP,
317 psc-QF>Tom, QS^{5A}/CyO-GFP with w^{1118}. Larvae were treated as in panel E but without the
318 temperature shift.

319 D. An example of a wing disc with GFP clones. The genotype was $GAL80^{5B}$/+; Act-GAL4,
320 UAS-GFP/+ from the cross of $GAL80^{5B}$/$GAL80^{5B}$ with Act-GAL4, UAS-GFP/CyO RFP Tb. Larvae
321 were treated as in panel E but without the temperature shift.

322 E. The experimental protocol used to express RNAi and transgenes conditionally in the
323 focused screen. For experiments that do not involve transgene expression, the same protocol
324 was followed but larvae were maintained at 25°C without a temperature shift.

325 F. Chromosomal location of QS^{5A}, QS^{9B}, *mwh* and GAL80 studied here (not to scale).

326 Scale bar = 120 microns in C-D.

327

328 **Fig 2. IR-induced LOH shows sex-dependence but locus-independence**

329 Larvae were treated as in Fig 1E but without the temperature shift and wing discs were fixed
330 and stained for DNA. The graphs show data are from at least two biological replicates per
331 sample, with the total number of wing discs examined for each sample is shown in parentheses.
332 Error bars represent mean±1 SEM. Scale bar = 120 microns. p-values were calculated using a 2-
333 tailed t-test.

334 (A-B) QS^{9B} and QS^{5A} are not significantly different in IR-induced LOH clone number (A) or
335 clone area (B).

336 (C-F) Quantification of GFP+ clone number (C-D) and clone area (E-F) with and without
337 irradiation for four GAL80 insertions on the X chromosome. Male and female larvae were
338 separated before dissection and processed separately.

339 (G-H) Quantification of GFP+ clone number (G) and clone area (H) with and without
340 irradiation for 12C6 GAL80 insertion on the X chromosome. Male and female larvae were
341 separated before dissection and processed separately.

342 (I-L) Representative examples of wing discs for the 12C insertion.

343 The genotypes were:

344 9B = psc-QF>Tom/+; QS^{9B}/+ that results from psc-QF>Tom; QS^{9B} X to w^{1118}

345 5A = psc-QF>Tom/QS^{5A} that results from psc-QF>Tom/CyO-GFP X QS^{5A}/CyO-GFP

346 (C-L) GAL80/+; Act-GAL4, UAS-GFP/+ that result from GAL80/GAL80 X Act-GAL4, UAS-
347 GFP/CyO RFP Tb
348
349 **Fig 3. A focused screen identified E2F1 as a regulator of LOH**
350 Wing discs from 3rd instar larvae were dissected 3 days after irradiation, fixed and stained for
351 DNA. Larvae were treated as in Fig 1E. The graphs show data from at least two biological
352 replicates per sample, with the total number of wing discs examined per sample shown in
353 parentheses. The mean±1 SEM is shown for each sample. p-values were calculated using a
354 paired 2-tailed t-test.
355 (A-B) Results of the focused screen showing clone number (A) and clone area (B). RNAi
356 against w is shown as the control for RNAi constructs and w^{1118} is shown as the control for
357 overexpression constructs.
358 (C-D') Representative examples of wing discs expressing $E2F1^{RNAi}$ or RAS^{V12} in the P
359 compartment (GFP+).
360
361 **Fig 4. Cell autonomous requirements for LOH**
362 (A-D) Larvae were treated as in Fig 1E but without the temperature shift and wing discs
363 were fixed and stained to visualize DNA. The discs shown are from irradiated larvae.
364 (E-F) Quantification of Tom+ clone number (E) and clone area (F) in irradiated discs. The
365 graphs show data from at least two biological replicates per sample, with the total number of
366 wing discs examined per sample shown in parentheses. The mean±1 SEM is shown for each
367 sample. p-values relative to w^{1118} controls were calculated using a 2-tailed t-test.
368 (G-I) Larvae were cultured and irradiated as in (A-F) but wing discs were dissected 4h
369 after IR, fixed and stained for DNA and with an antibody against cleaved active Dcp1 as a
370 surrogate marker for apoptosis.
371 Scale bars = 120 microns.
372 The genotypes are as shown below. Stock information is in Supplemental Table 1.
373 (A,G) Control = psc-QF>Tom/+; QS^{9B}/+ that results from psc-QF>Tom; QS^{9B} X to w^{1118}
374 (H-I) psc-QF>Tom/QUAS-transgene; QS^{9B}/+
375 (B-D) psc-QF>Tom/+; QS^{9B}/QUAS-transgene
376

377 **References**

378 Baker, B. S., A. T. Carpenter and P. Ripoll, 1978 The Utilization during Mitotic Cell Division of
379 Loci Controlling Meiotic Recombination and Disjunction in DROSOPHILA
380 MELANOGASTER. Genetics 90**:** 531-578.
381 Brodsky, M. H., B. T. Weinert, G. Tsang, Y. S. Rong, N. M. McGinnis *et al.*, 2004 Drosophila
382 melanogaster MNK/Chk2 and p53 regulate multiple DNA repair and apoptotic pathways
383 following DNA damage. Mol Cell Biol 24**:** 1219-1231.
384 Brown, J., I. Bush, J. Bozon and T. T. Su, 2020 Cells with loss-of-heterozygosity after exposure to
385 ionizing radiation in Drosophila are culled by p53-dependent and p53-independent
386 mechanisms. PLoS Genet 16**:** e1009056.
387 Charan, J., and N. D. Kantharia, 2013 How to calculate sample size in animal studies? J
388 Pharmacol Pharmacother 4**:** 303-306.
389 Chick, W. S., S. E. Mentzer, D. A. Carpenter, E. M. Rinchik, D. Johnson *et al.*, 2005 X-ray-induced
390 deletion complexes in embryonic stem cells on mouse chromosome 15. Mamm Genome
391 16**:** 661-671.
392 Eeken, J. C., A. W. de Jong, M. Loos, C. Vreeken, R. Romeyn *et al.*, 1994 The nature of X-ray-
393 induced mutations in mature sperm and spermatogonial cells of Drosophila
394 melanogaster. Mutat Res 307**:** 201-212.
395 Goupil, A., J. P. Heinen, R. Salame, F. Rossi, J. Reina *et al.*, 2022 Illuminati: a form of gene
396 expression plasticity in Drosophila neural stem cells. Development 149.
397 Kerkis, J., 1931 The Growth of the Gonads in DROSOPHILA MELANOGASTER. Genetics 16**:** 212-
398 224.
399 Kurzhals, R. L., L. Fanti, A. C. G. Ebsen, Y. S. Rong, S. Pimpinelli *et al.*, 2017 Chromosome Healing
400 Is Promoted by the Telomere Cap Component Hiphop in Drosophila. Genetics 207**:** 949-
401 959.
402 Lawrence, P. A., B. Sanson and J. P. Vincent, 1996 Compartments, wingless and engrailed:
403 patterning the ventral epidermis of Drosophila embryos. Development 122**:** 4095-4103.
404 Martin-Blanco, E., A. Gampel, J. Ring, K. Virdee, N. Kirov *et al.*, 1998 puckered encodes a
405 phosphatase that mediates a feedback loop regulating JNK activity during dorsal closure
406 in Drosophila. Genes Dev 12**:** 557-570.
407 McNamee, L. M., and M. H. Brodsky, 2009 p53-independent apoptosis limits DNA damage-
408 induced aneuploidy. Genetics 182**:** 423-435.
409 Pastink, A., A. P. Schalet, C. Vreeken, E. Paradi and J. C. Eeken, 1987 The nature of radiation-
410 induced mutations at the white locus of Drosophila melanogaster. Mutat Res 177**:** 101-
411 115.
412 Pastink, A., C. Vreeken, A. P. Schalet and J. C. Eeken, 1988 DNA sequence analysis of X-ray-
413 induced deletions at the white locus of Drosophila melanogaster. Mutat Res 207**:** 23-28.
414 Perez-Garijo, A., Y. Fuchs and H. Steller, 2013 Apoptotic cells can induce non-autonomous
415 apoptosis through the TNF pathway. Elife 2**:** e01004.
416 Reis, T., and B. A. Edgar, 2004 Negative regulation of dE2F1 by cyclin-dependent kinases
417 controls cell cycle timing. Cell 117**:** 253-264.
418 Riabinina, O., D. Luginbuhl, E. Marr, S. Liu, M. N. Wu *et al.*, 2015 Improved and expanded Q-
419 system reagents for genetic manipulations. Nat Methods 12**:** 219-222, 215 p following
420 222.

421 Siudeja, K., S. Nassari, L. Gervais, P. Skorski, S. Lameiras *et al.*, 2015 Frequent Somatic Mutation
422 in Adult Intestinal Stem Cells Drives Neoplasia and Genetic Mosaicism during Aging. Cell
423 Stem Cell 17**:** 663-674.
424 Wells, B. S., and L. A. Johnston, 2012 Maintenance of imaginal disc plasticity and regenerative
425 potential in Drosophila by p53. Dev Biol 361**:** 263-276.
426 Wichmann, A., B. Jaklevic and T. T. Su, 2006 Ionizing radiation induces caspase-dependent but
427 Chk2- and p53-independent cell death in Drosophila melanogaster. Proc Natl Acad Sci U
428 S A 103**:** 9952-9957.
429 zouabi, L. A., M. Stefanutti, N. Riddiford, N. Rubanova, M. Bohec *et al.*, 2022 Molecular
430 Underpinnings and Environmental Drivers of Spontaneous Loss of Heterozygosity in
431 Drosophila Intestinal Stem Cells. bioRxiv**:** 2022.2007.2021.500951.
432

Figure 1

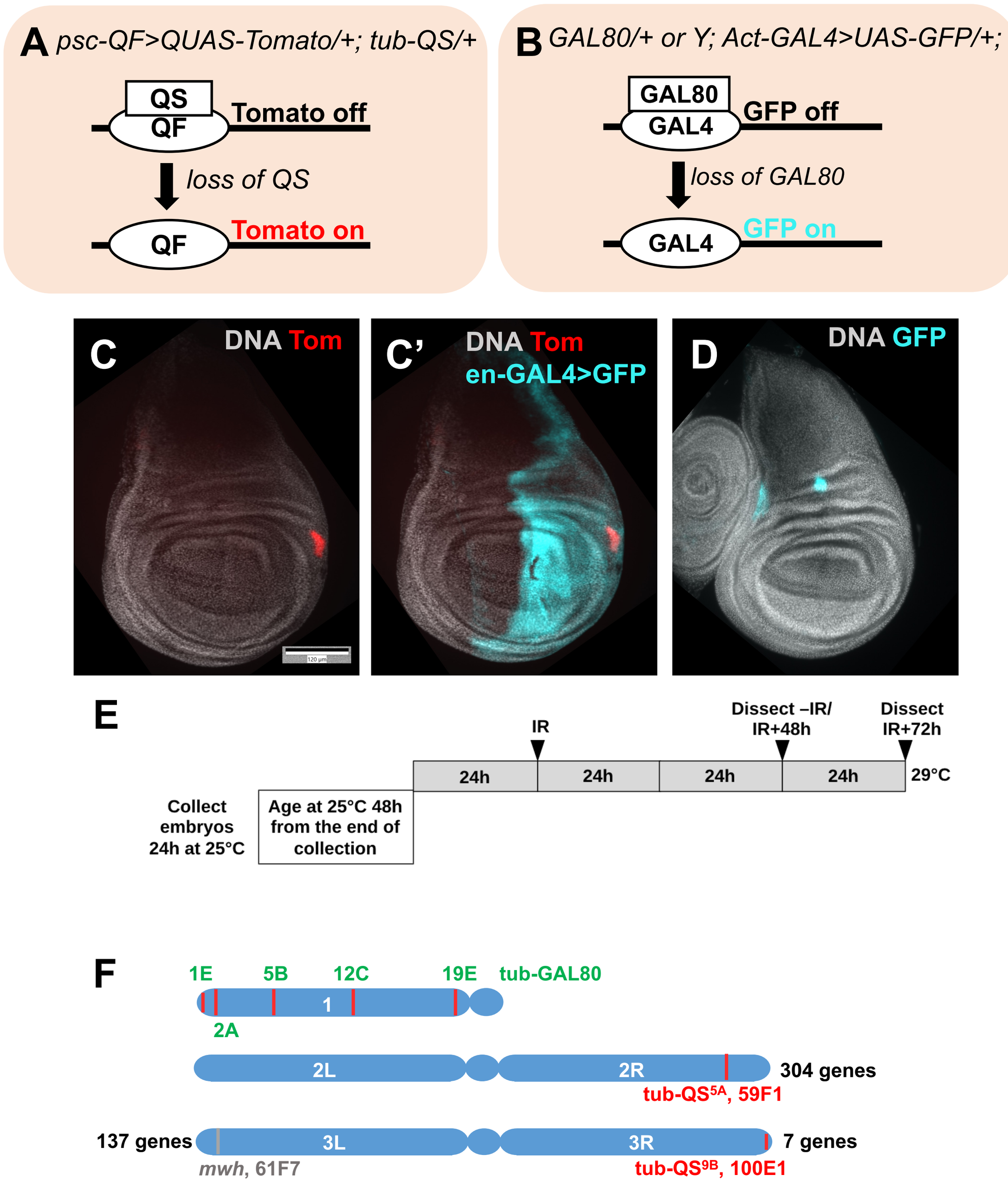
A psc-QF>QUAS-Tomato/+; tub-QS/+
QS
QF
Tomato off
loss of QS
QF
Tomato on
B GAL80/+ or Y; Act-GAL4>UAS-GFP/+;
GAL80
GAL4
GFP off
loss of GAL80
GAL4
GFP on
C
DNA Tom
120 µm
C'
DNA Tom
en-GAL4>GFP
D
DNA GFP
E
IR
Dissect –IR/
IR+48h
Dissect
IR+72h
24h
24h
24h
24h
29°C
Collect
embryos
24h at 25°C
Age at 25°C 48h
from the end of
collection
F
1E
5B
12C
19E
tub-GAL80
1
2A
2L
2R
304 genes
tub-QS5A, 59F1
137 genes
3L
3R
7 genes
mwh, 61F7
tub-QS9B, 100E1

Figure 2

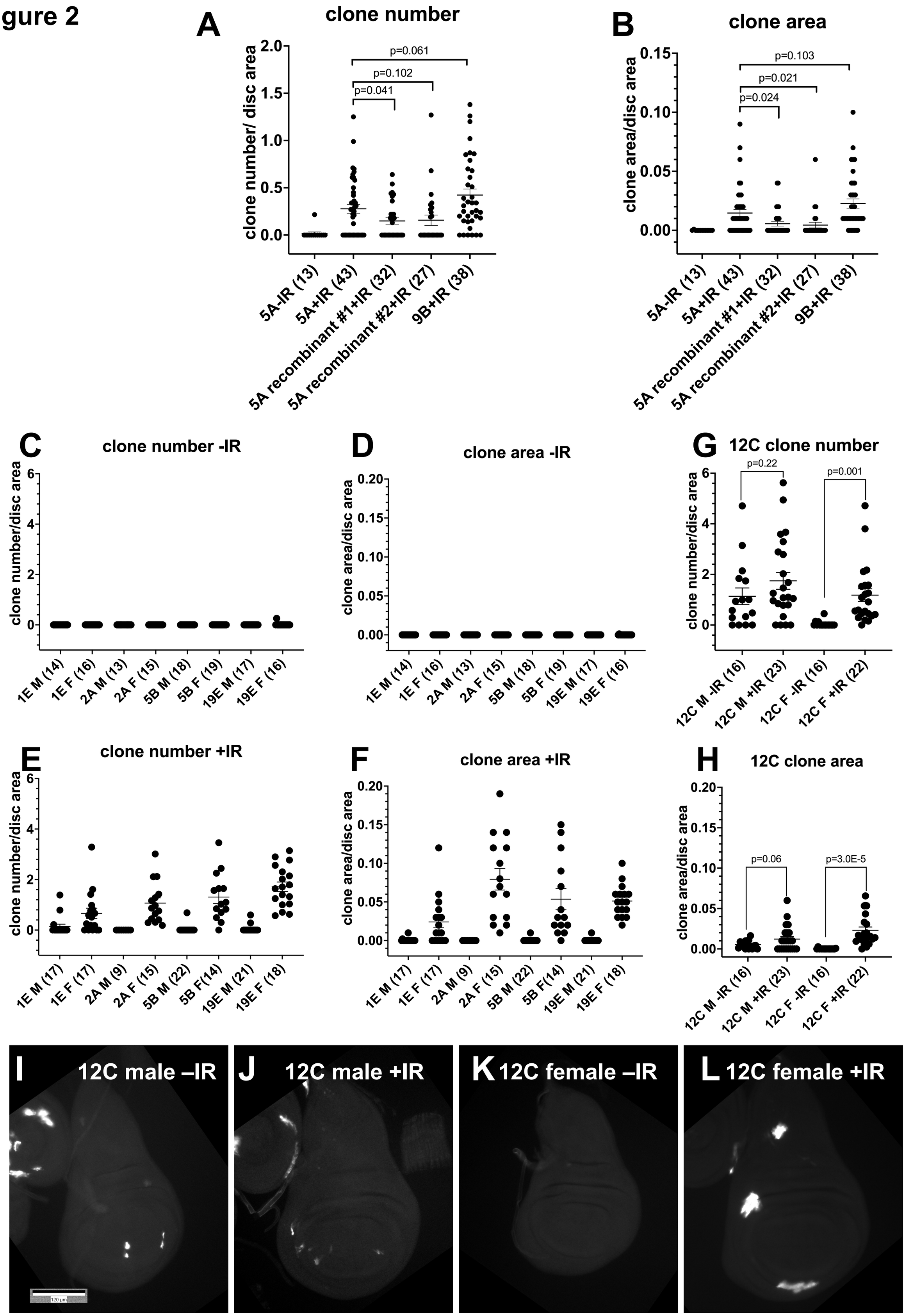
A
clone number
clone number/ disc area
p=0.061
p=0.102
p=0.041
5A-IR (13)
5A+IR (43)
5A recombinant #1+IR (32)
5A recombinant #2+IR (27)
9B+IR (38)
B
clone area
clone area/disc area
p=0.103
p=0.021
p=0.024
C
clone number -IR
D
clone area -IR
G
12C clone number
p=0.22
p=0.001
1E M (14)
1E F (16)
2A M (13)
2A F (15)
5B M (18)
5B F (19)
19E M (17)
19E F (16)
12C M -IR (16)
12C M +IR (23)
12C F -IR (16)
12C F +IR (22)
E
clone number +IR
F
clone area +IR
H
12C clone area
p=0.06
p=3.0E-5
1E M (17)
1E F (17)
2A M (9)
2A F (15)
5B M (22)
5B F(14)
19E M (21)
19E F (18)
I
12C male –IR
J
12C male +IR
K
12C female –IR
L
12C female +IR
120 µm

Figure 3

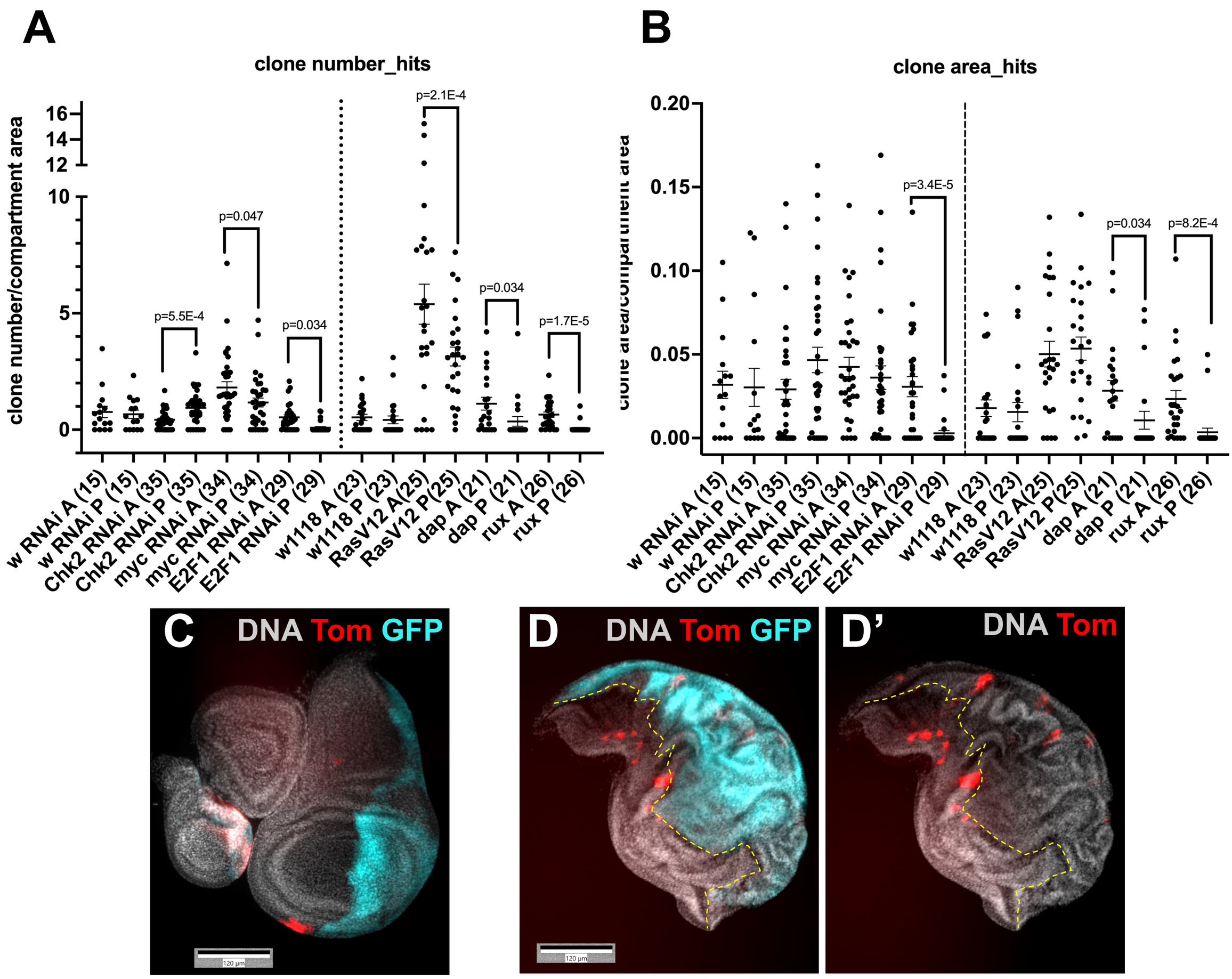
A
clone number_hits
clone number/compartment area
16
14
12
10
5
0
p=5.5E-4
p=0.047
p=0.034
p=2.1E-4
p=0.034
p=1.7E-5
w RNAi A (15)
w RNAi P (15)
Chk2 RNAi A (35)
Chk2 RNAi P (35)
myc RNAi A (34)
myc RNAi P (34)
E2F1 RNAi A (29)
E2F1 RNAi P (29)
w1118 A (23)
w1118 P (23)
RasV12 A(25)
RasV12 P(25)
dap A (21)
dap P (21)
rux A (26)
rux P (26)
B
clone area_hits
clone area/compartment area
0.20
0.15
0.10
0.05
0.00
p=3.4E-5
p=0.034
p=8.2E-4
C
DNA Tom GFP
120 µm
D
DNA Tom GFP
120 µm
D'
DNA Tom
E2F1 RNAi
RASV12

Figure 4

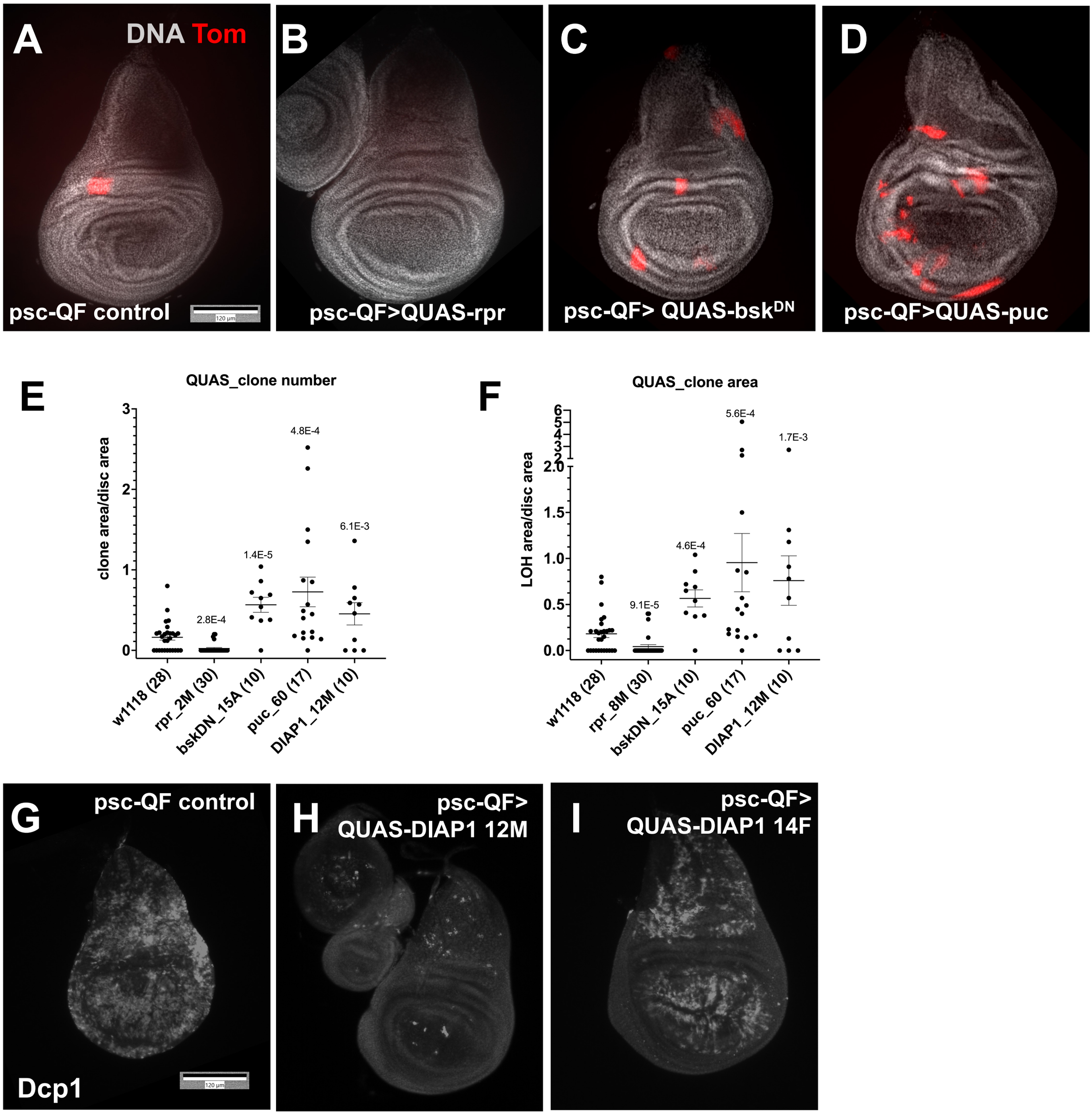
A
DNA Tom
psc-QF control
120 µm
B
psc-QF>QUAS-rpr
C
psc-QF> QUAS-bskDN
D
psc-QF>QUAS-puc
E
QUAS_clone number
clone area/disc area
0
1
2
3
2.8E-4
1.4E-5
4.8E-4
6.1E-3
w1118 (28)
rpr_2M (30)
bskDN_15A (10)
puc_60 (17)
DIAP1_12M (10)
F
QUAS_clone area
LOH area/disc area
0.0
0.5
1.0
1.5
2.0
2
3
4
5
6
9.1E-5
4.6E-4
5.6E-4
1.7E-3
w1118 (28)
rpr_8M (30)
bskDN_15A (10)
puc_60 (17)
DIAP1_12M (10)
G
psc-QF control
Dcp1
120 µm
H
psc-QF>
QUAS-DIAP1 12M
I
psc-QF>
QUAS-DIAP1 14F

Supplemental Figure 1

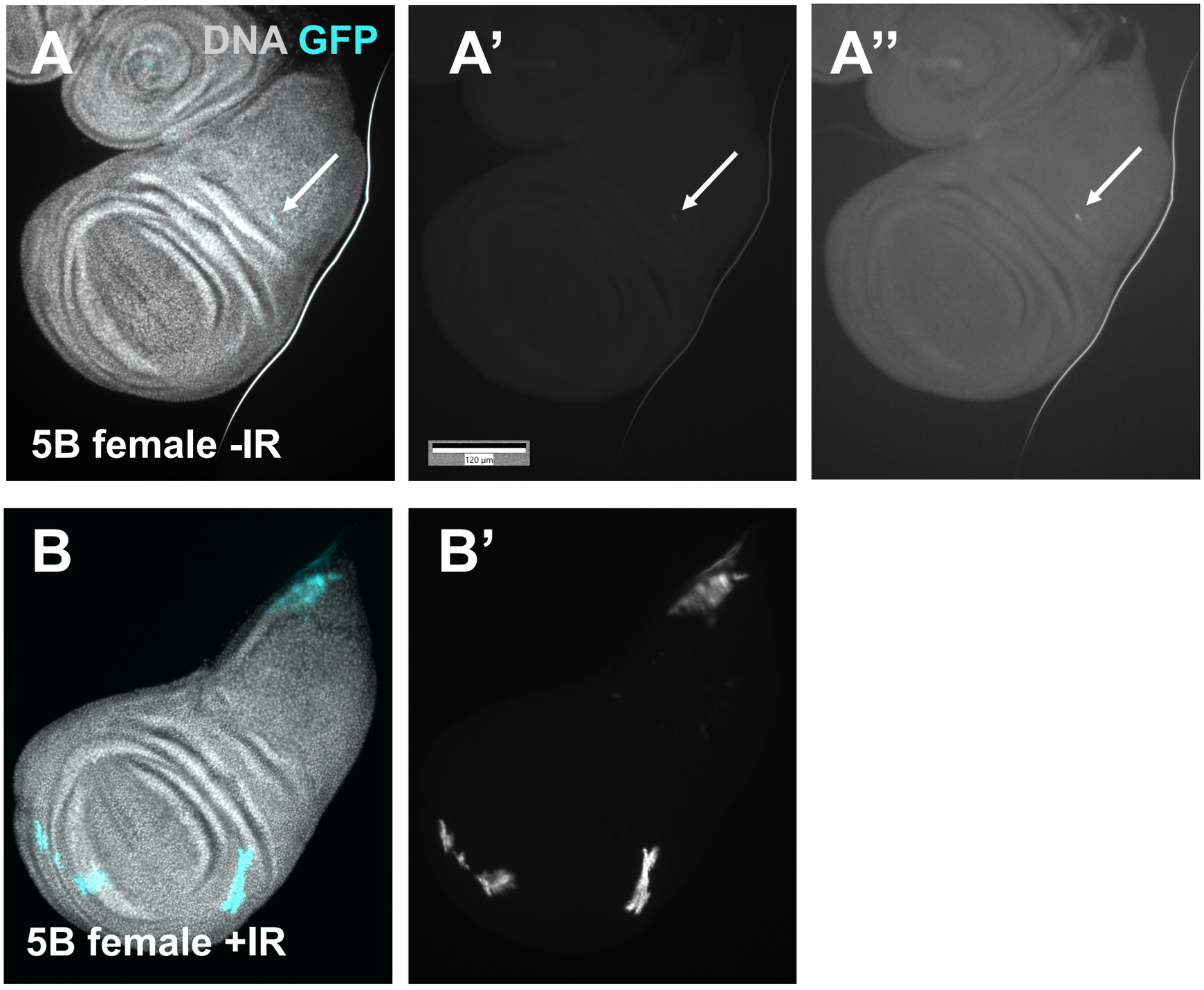

Supplemental Figure 1. Spontaneous GFP is less bright than IR-induced GFP.
Larvae were treated as in Fig 1E but without the temperature shift and wing discs were fixed and stained to visualize DNA. The genotype of the larvae was GAL80^{5B}/+; Act-GAL4, UAS-GFP/+ from the cross of GAL80^{5B}/GAL80^{5B} with Act-GAL4, UAS-GFP/CyO RFP Tb.

(A-A''') A disc from an unirradiated larva showing one faint GFP spot (arrow).

(B-B') A disc from an irradiated larva showing bright GFP spots. A' and B' are shown with similar brightness and contrast range in ImageJ so that signals would be directly comparable. A'' is shown with a narrower range to allow the viewer to see the faint GFP spot.

Supplemental Figure 2

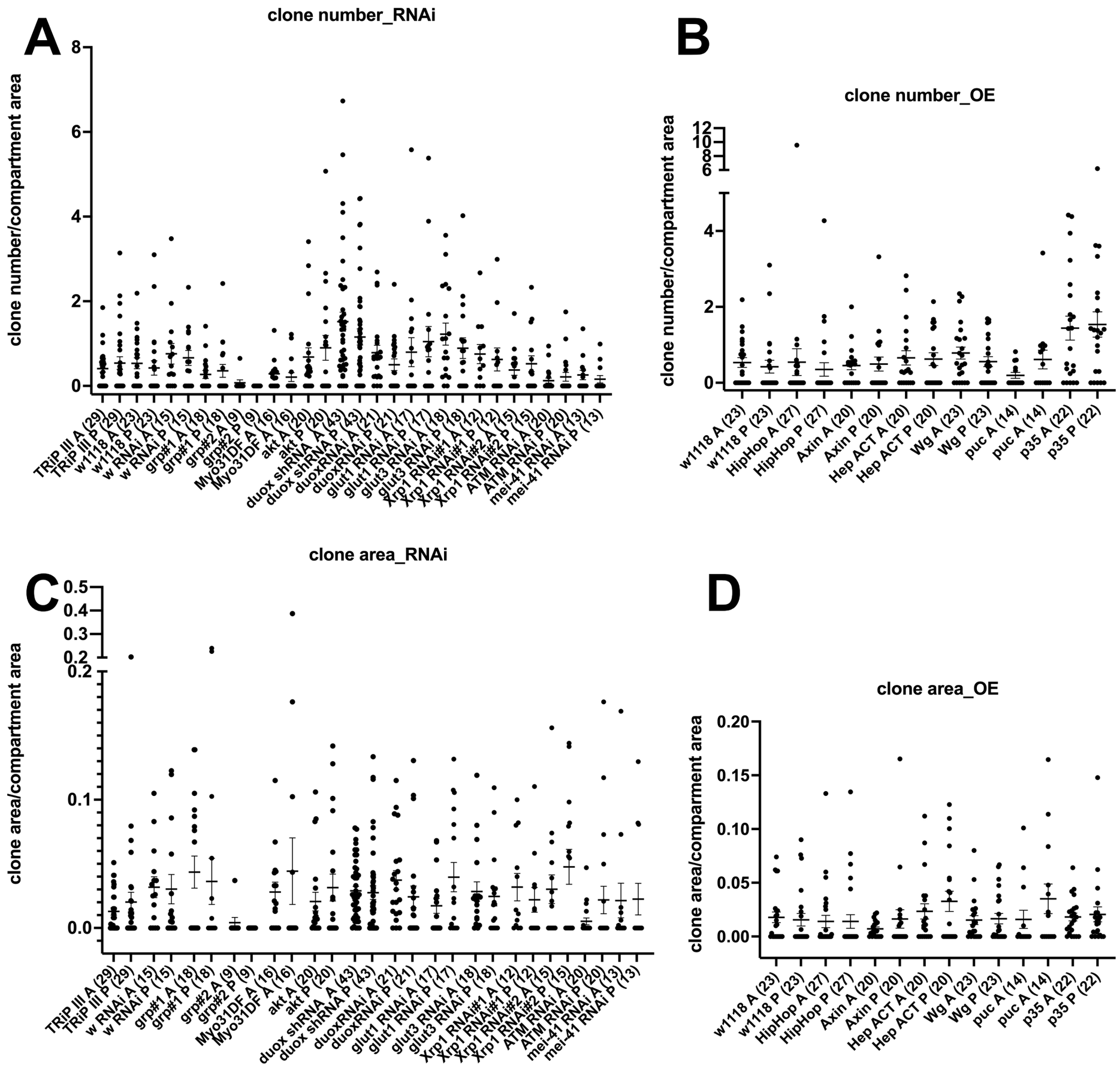

Supplemental Figure 2. A focused screen for modulators of IR-induced QS^{9B} LOH.
Wing discs from 3rd instar larvae were dissected 3 days after irradiation, fixed, and stained for DNA. Larvae were treated as in Fig 1E. The graphs show data from at least two biological replicates per sample, with the total number of wing discs examined per sample shown in parentheses. The mean±1 SEM is shown for each sample. Because A and P compartments are of different sizes, clone numbers and clone areas have been normalized to compartment area. p-values between A and P samples for each genotype (none <0.05) were calculated using a paired 2-tailed t-test. TRiP III (background stock for most RNAi lines used) and RNAi against w served as controls for RNAi constructs and w^{1118} served as the control for overexpression constructs.

(A-B) LOH clone numbers for RNAi (A) and overexpression (OE,B) constructs.

(C-D) LOH clone areas for RNAi (C) and overexpression (OE,D) constructs.

Supplemental Table 1

Supplemental Table 1. Drosophila stocks used in this work					
I. General stocks (BL = Bloomington Stock Center)					
stock #/source	*used in Fig.*	*used for*	*genotype*		
BL30042	Fig 2-4, S1	monitor LOH of QS{9B}	y[1] w[1118]; P{w[+mC]=M2ET-QF}ET40, P{w[+mC]=QUAS-mtdTomato-3xHA}CP; P{ry[+t7.2]=neoFRT}82B P{w[+mC]=tub-QS.P}9B		
BL30133	Fig 1-2	monitor LOH of QS{5A}	y[1] w[1118]; P{w[+mW.hs]=FRT(w[hs])}G13 P{w[+mC]=tub-QS.P}5A		
BL30043	Fig 1-4, S1, Table S2	expresses Tom throughout the wing disc	y[1] w[1118]; P{w[+mC]=QUAS-mtdTomato-3xHA}14 P{w[+mC]=M2ET-QF}ET40/CyO		
unknown	Fig 1, 3, S2	P compartment expression	engrailed-GAL4 on chromosome II		
BL5431	Fig 1, 3, S2	mark the P compartment	UAS-eGFP on chromosome II		
Bardin lab	Fig 2	detecting loss of GAL80	Actin-GAL4, UAS-GFP		
II. Stocks used in the focused screen and for functional testing (VDRC = Vienna Drosophila Resource Center)					
gene	*function*	*construct*	*manipulation*	*stock #*	*ref./source*
p35	anti-apoptotic	UAS-p35	overexpression	BL5073	Bloomington Stock Center
Diap1	anti-apoptotic	QUAS-DIAP1	overexpression	N/A	Steller lab
rpr	pro-apoptotic	QUAS-rpr	overexpression	N/A	Perez-Garijo et a., 2013
E2F1	cell cycle, apoptosis	UAS-dsRNA	RNAi	BL27564	Bloomington Stock Center
rux	inhibits mitotic Cdk	UAS-Rux	overexpression	BL9166	Bloomington Stock Center
dap	inhibits G1/S Cdk	UAS-Dap	overexpression	BL83334	Bloomington Stock Center
tefu/ATM	DNA damage response	UAS-dsRNA	RNAi	V22502	VDRC
mei-41/ATR	DNA damage response	UAS-dsRNA	RNAi	v11251	VDRC
grp/Chk1	DNA damage response	UAS-dsRNA	RNAi (GL00067)	N/A	Perrimon lab
grp/Chk1#2	DNA damage response	UAS-dsRNA	RNAi (HMS01573)	BL36685	Bloomington Stock Center
loki/Chk2	DNA damage response	UAS-dsRNA	RNAi	BL35152	Bloomington Stock Center
hiphop	chromosome end healing	P{EPgy2} insertion	overexpression	BL17618	Bloomington Stock Center
Puc	represses JNK signaling	UAS-puc	overexpression	N/A	Martin-Blanco et al., 1998
Puc	represses JNK signaling	QUAS-puc	overexpression	N/A	Steller lab
Bsk/JNK	stress response	QUAS-JNK DN	dominant negative	N/A	Steller lab
hep/JNKK	Stress response	UAS-hep ACT	constitutively active	BL9306	Bloomington Stock Center
Akt	Stress response	UAS-dsRNA	RNAi	BL31701	Bloomington Stock Center
myc	Growth	UAS-dsRNA	RNAi	v2947	VDRC
Ras	Growth, apoptosis	UAS-RAS V12 mutant	constitutively active	BL64195	Bloomington Stock Center
wg/Wnt1	Developmental signaling	UAS	overexpression	N/A	Lawrence et al., 1996
Axin	inhibits Wg signaling	UAS-Axin	overexpression	BL7225	Bloomington Stock Center
duox	Cell competition	UAS-dsRNA	RNAi	BL33975	Bloomington Stock Center
duox	Cell competition	UAS-shRNA	shRNA	v330085	VDRC
Myo31DF	Cell competition	UAS-dsRNA	RNAi	BL33971	Bloomington Stock Center
Xrp1	Cell competition	UAS-dsRNA	RNAi	v107860	VDRC
glut1	p53 target	UAS-dsRNA	RNAi	v13326	VDRC
glut3	p53 target	UAS-dsRNA	RNAi	v13302	VDRC
w	control	UAS-dsRNA	RNAi	BL33623	Bloomington Stock Center
TRiP III	control stock for RNAi lines	N/A	none	BL36303	Bloomington Stock Center
w1118	control	none	none	BL3605	Bloomington Stock Center

Supplemental Table 2

Supplemental Table 2. X2 test for survival after ubiquitous expression of QUAS transgenes.													
Psc-QF, mtdTomato/CyO-GFP virgins crossed to	tested stock (stock#)	inserted Chromosome	Cy	Cy+	GFP-	GFP+	total	expected Cy or GFP-	expected Cy+ or GFP-	(o-e)^2	(o-e)^2	X2	p
N/A	**w1118 control**		**38**	**50**			**88**	**44**	**44**	**36.0**	**36.0**	**1.6**	**n.s.**
QUAS-X/CyO; Sb/TM6 Tb	QUAS-rpr (11M)	2	88	0	N/A	N/A	88	44	44	1936.0	1936.0	88.0	<0.001
QUAS-X/CyO; Sb/TM6 Tb	QUAS-rpr (12M)	2	58	0	N/A	N/A	58	29	29	841.0	841.0	58.0	<0.001
Sco/CyO; QUAS-X/TM6 Tb	**QUAS-rpr (2M)**	**3**	**N/A**	**N/A**	**0**	**47**	**47**	**31**	**16**	**981.8**	**981.8**	**94.0**	**<0.001**
QUAS-X/CyO; Sb/TM6 Tb	QUAS-DIAP1 (3M)	2	34	14	N/A	N/A	48	24	24	100.0	100.0	8.3	<0.005
QUAS-X/CyO; Sb/TM6 Tb	QUAS-DIAP1 (8M)	2	64	24	N/A	N/A	88	44	44	400.0	400.0	18.2	<0.001
QUAS-X/CyO; Sb/TM6 Tb	**QUAS-DIAP1 (12M)**	**2**	**49**	**61**	**N/A**	**N/A**	**110**	**55**	**55**	**36.0**	**36.0**	**1.3**	**n.s.**
QUAS-X/CyO; Sb/TM6 Tb	QUAS-bskDN (19)	2	38	0	N/A	N/A	38	19	19	361.0	361.0	38.0	<0.001
Sco/CyO; QUAS-X/TM6 Tb	**QUAS-bskDN (15A)***	**3**	**N/A**	**N/A**	**0**	**25**	**25**	**17**	**8**	**277.8**	**277.8**	**50.0**	**<0.001**
Sco/CyO; QUAS-X/TM6 Tb	QUAS-bskDN (30)	3	N/A	N/A	4	19	23	15	8	128.4	128.4	25.1	<0.001
Sco/CyO; QUAS-X/TM6 Tb	QUAS-bskDN (43)	3	N/A	N/A	2	13	15	10	5	64.0	64.0	19.2	<0.001
QUAS-X/CyO; Sb/TM6 Tb	QUAS-puc (21)	2	30	0	N/A	N/A	30	15	15	225.0	225.0	30.0	<0.001
QUAS-X/CyO; Sb/TM6 Tb	QUAS-puc (66)	2	72	10	N/A	N/A	82	41	41	961.0	961.0	46.9	<0.001
Sco/CyO; QUAS-X/TM6 Tb	QUAS-puc (59)	3	N/A	N/A	0	12	12	8	4	64.0	64.0	24.0	<0.001
Sco/CyO; QUAS-X/TM6 Tb	**QUAS-puc (60)**	**3**	**N/A**	**N/A**	**0**	**16**	**16**	**11**	**5**	**113.8**	**113.8**	**32.0**	**<0.001**
*counted as pupa													

Supplemental Table 2. X^2 test for survival after ubiquitous expression of QUAS transgenes. For chromosome 2 lines, CyO balancer was floating so Cy+ males were used. Male QUAS flies were crossed to virgins of the genotype psc-QF>UAS-Tomato/CyO-GFP. Embryos were collected overnight. CyO and CyO+ progenies were counted until no new adults eclosed for a 24 h period. X^2 test was used to assess deviations from the 1:1 expected Mendelian ratio. For insertions on chromosome 3, Tb+ pupae were sorted and scored as GFP+ or GFP- before eclosion was monitored. X^2 test was used to assess deviations from the 2GFP- (Sco/QF>Tom and QF>Tom/CyO):1GFP+ (Sco/CyO-GFP) expected Mendelian ratio.